

## Supporting Information

### Manganese-promoted cleavage of acetylacetonate resembling the $\beta$ -diketone cleaving dioxygenase (Dke1) reactivity

Chao Yang, Dingqi Liu, Tongshuai Wang, Fuxing Sun, Shilun Qiu and Gang Wu\*

#### Experimental section

##### Materials and methods

All chemicals were obtained commercially without further purification.

Elemental analysis (C, H and N) was carried out using a Perkin-Elmer 2400 Elemental Analyzer.  $^1\text{H}$  NMR spectra were recorded in deuterated DMSO with a 300 MHz Mercury Varian-300 NMR spectrometer. IR spectra were recorded in the range 400-4000  $\text{cm}^{-1}$  with a Bruker IFS 66v/S IR spectrometer using KBr pellets. The UV-visible spectra were got from UV/VIS spectrophotometer (Shimadzu UV-2450). The magnetic measurements were carried out with a Quantum Design MPMS-XL7 SQUID magnetometer using a polycrystalline sample. Magnetic susceptibility data were obtained from 300 K to 2 K at a 1000 Oe dc field and field-dependent magnetization plots were drawn between 2K for applied fields ranging from 0 to 60 kOe. GC-MS was carried out using a Shimadzu GCMS-QP2010 Plus with a flame ionization detector (FID). The column was GsBP-1 ms (0.25 mm  $\times$  30 m  $\times$  0.25  $\mu\text{m}$ ); the initial temperature was 60  $^\circ\text{C}$ , the heating rate was 10  $^\circ\text{C min}^{-1}$ , and the final temperature was 280  $^\circ\text{C}$ , the temperature of the FID detector was 250  $^\circ\text{C}$ . Crystallographic analysis was performed in the ambient condition. Space groups were identified based on XPREP implemented in APEX II. The crystalline structure was worked out through direct methods (SHELXT).<sup>1</sup> The positions of metal atoms were confirmed first, and then the oxygen and carbon atoms of the crystal were located on account of difference Fourier maps. Full-matrix least-squares on  $F^2$  was accomplished to refine non-hydrogen atoms using SHELXL-2018/3.<sup>2</sup> All the non-hydrogen atoms were refined with anisotropic parameters. The presence of large regions of diffuse electron density that could not be modeled, accounting for the remaining solvent molecules, required use of the "Solvent Mask" function in the OLEX-2 software package.<sup>3</sup>

##### Synthesis

2-(hydroxy(bipyridin-2-yl)methyl)phenol ( $\text{H}_2\text{L}_2$ ) and 2-benzyloxybromo-benzene was synthesized according to the literature.<sup>4</sup>  $^1\text{H}$  NMR (300 MHz, DMSO- $d_6$ , 25  $^\circ\text{C}$ )  $\delta$  11.12 (s, 1H), 8.45 (ddd,  $J = 4.8, 1.8, 0.9$  Hz, 2H), 7.83 (ddd,  $J = 8.0, 7.5, 1.8$  Hz, 2H), 7.51 (dt,  $J = 8.0, 1.0$  Hz, 2H), 7.45 (dd,  $J = 7.8, 1.7$  Hz, 1H), 7.31 (ddd,  $J = 7.5, 4.8, 1.1$  Hz, 2H), 7.15 (ddd,  $J = 7.9, 7.3, 1.7$  Hz, 1H), 6.82 (ddd,  $J = 7.8, 7.3, 1.3$  Hz, 2H), 6.74 (dd,  $J = 8.0, 1.2$  Hz, 1H). (Fig. S5)

### Synthesis of (2-(benzyloxy)phenyl)(pyridin-2-yl)methanol.

A 250 mL double-necked round bottom flask was charged with magnesium (2.67 g, 110 mmol), the catalytic amount of iodine, and dried THF (150 mL). Then corresponding 2-benzyloxybromo-benzene (28.9 g, 110 mmol) was added with vigorously stirring, treated with a heat gun and the colour of iodine disappeared slowly on time, indicating the generation of Grignard reagent<sup>5</sup>. It was stirred for 2h followed by the addition of picolinaldehyde (10.7 g, 100 mmol). The mixture was then stirred for 1h. Completion of reaction was monitored by TLC analysis. Saturated aqueous NH<sub>4</sub>Cl (50 mL) was added to quench the reaction and the aqueous phase was extracted by EtOAc (50 mL×3). The combined organic phase was dried over anhydrous Na<sub>2</sub>SO<sub>4</sub>, filtered, and concentrated under reduced pressure. The crude product was purified by column chromatography on silica gel (petroleum ether/EtOAc, 6:1). The product was dried overnight under vacuum to afford (2-(benzyloxy)phenyl)(pyridin-2-yl)methanol as a light yellow liquid. Yield: 27.1 g, 93%. <sup>1</sup>H NMR (300 MHz, DMSO-d<sub>6</sub>, 25 °C) δ 8.45 (ddd, *J* = 4.8, 1.8, 0.9 Hz, 1H), 7.72 (td, *J* = 7.7, 1.8 Hz, 1H), 7.44 – 7.37 (m, 2H), 7.37 – 7.27 (m, 5H), 7.25 – 7.14 (m, 2H), 7.01 (dd, *J* = 8.3, 0.9 Hz, 1H), 6.94 (td, *J* = 7.4, 1.0 Hz, 1H), 6.09 (d, *J* = 5.1 Hz, 1H), 5.83 (d, *J* = 5.1 Hz, 1H), 5.08 (s, 2H). (Fig. S1)

### Synthesis of (2-(benzyloxy)phenyl)(pyridin-2-yl)methanone.

(2-(benzyloxy)phenyl)(pyridin-2-yl)methanol (26.2g, 90mmol) was solved in DCM (300mL), followed by addition of PCC (38.8g, 180mmol) in slowly, and stirred for 4h in room temperature. Completion of reaction was monitored by TLC analysis. The mixture was filtered with kieselguhr and the filtrate was under reduced pressure to remove the solvent. The crude product was purified by column chromatography on silica gel (petroleum ether/EtOAc, 6:1). The product was dried overnight under vacuum to afford (2-(benzyloxy)phenyl)(pyridin-2-yl)methanone as a light yellow solid. Yield: 24.7g, 95%. <sup>1</sup>H NMR (300 MHz, DMSO-d<sub>6</sub>, 25 °C) δ 8.61 (ddd, *J* = 4.7, 1.7, 0.9 Hz, 1H), 8.04 – 7.95 (m, 1H), 7.95 – 7.87 (m, 1H), 7.59 (ddd, *J* = 7.5, 4.8, 1.4 Hz, 1H), 7.56 – 7.50 (m, 1H), 7.46 (dd, *J* = 7.5, 1.7 Hz, 1H), 7.23 – 7.16 (m, 4H), 7.10 (td, *J* = 7.4, 0.9 Hz, 1H), 6.88 (dt, *J* = 4.2, 3.3 Hz, 2H), 4.98 (s, 2H). (Fig. S2)

### Synthesis of bis(2-(benzyloxy)phenyl)(pyridin-2-yl)methanol.

The generation of Grignard reagent of 2-benzyloxybromo-benzene was same to above mentioned. Then (2-(benzyloxy)phenyl)(pyridin-2-yl)methanone (23.1g, 80mmol) was added and stirred for 4h. Saturated aqueous NH<sub>4</sub>Cl (50 mL) was added to quench the reaction and the aqueous phase was extracted by EtOAc (50 mL×3). The combined organic phase was dried over anhydrous Na<sub>2</sub>SO<sub>4</sub>, filtered, and concentrated under reduced pressure. The crude product was purified by column chromatography on silica gel (petroleum ether/EtOAc, 3:1). The product was dried overnight under vacuum to afford bis(2-(benzyloxy)phenyl)(pyridin-2-yl)methanol as a light yellow solid. Yield: 33.7 g, 89%. <sup>1</sup>H NMR (300 MHz, DMSO-d<sub>6</sub>, 25 °C) δ 8.39 (ddd, *J* = 4.8, 1.8, 0.9 Hz, 1H), 7.56 – 7.45 (m, 1H), 7.40 – 7.33 (m, 1H), 7.27 (tt, *J* = 10.6, 2.5 Hz, 2H), 7.23 – 7.10 (m, 9H), 7.05 (dd, *J* = 8.2, 1.0 Hz, 2H), 6.97 – 6.80 (m, 6H), 6.03 (s, 1H), 4.99 – 4.77 (m, 4H). (Fig. S3)

### Synthesis of 2,2'-(hydroxy(pyridin-2-yl)methylene)diphenol (H<sub>3</sub>L<sub>1</sub>).

Bis(2-(benzyloxy)phenyl)(pyridin-2-yl)methanol (33.1g, 70mmol) was solved in MeOH and flushed with Ar and H<sub>2</sub> in sequence. The mixture was stirred in H<sub>2</sub> ambient until the reaction was completed, monitored by TLC. After removing the solvent by reduced pressure, the crude product was purified by column chromatography on silica gel (petroleum ether/EtOAc, 1:1) to give white powder product. Yield: 19.9g, 97%. <sup>1</sup>H NMR (300 MHz, DMSO-d<sub>6</sub>, 25 °C) δ 10.02 (s, 2H), 8.48 – 8.34 (m, 1H), 7.94 – 7.81 (m, 1H), 7.76 (d, *J* = 8.0 Hz, 1H), 7.30 (ddd, *J* = 7.3, 4.9, 1.2 Hz, 1H), 7.23 – 7.08 (m, 2H), 7.07 – 6.95 (m, 2H), 6.84 – 6.66 (m, 4H), 6.58 (s, 1H). (Fig. S4)

#### **Synthesis of 2,2',2''-(hydroxymethanetriyl)triphenol (H<sub>4</sub>L<sub>3</sub>).**

The synthesis procedure of H<sub>4</sub>L<sub>3</sub> (Scheme S2) was similar to H<sub>3</sub>L<sub>1</sub> (Scheme S1), while the initial substrate was replaced with 2-(benzyloxy)benzaldehyde. <sup>1</sup>H NMR (300 MHz, DMSO-d<sub>6</sub>, 25 °C) δ 9.45 (s, 3H), 7.19 (ddd, *J* = 8.0, 7.3, 1.7 Hz, 3H), 6.85 (dd, *J* = 8.1, 1.2 Hz, 3H), 6.71 (td, *J* = 7.5, 1.2 Hz, 3H), 6.47 (dd, *J* = 7.8, 1.6 Hz, 3H). (Fig. S6)

#### **Preparation of [Mn<sup>III</sup><sub>4</sub>Mn<sup>II</sup><sub>2</sub>K<sub>2</sub>(L<sub>1</sub>)<sub>4</sub>(HL<sub>1</sub>)<sub>2</sub>(oxa)(H<sub>2</sub>O)<sub>4</sub>]·(solvent)<sub>x</sub> (compound 1)**

Mn(acac)<sub>3</sub> (317mg, 0.9mmol), H<sub>3</sub>L<sub>1</sub> (176mg, 0.6mmol), and KHCO<sub>3</sub> (180mg, 1.8mmol) were solved in CH<sub>3</sub>OH (20mL). After stirring for 5 h, the resulting dark solution was filtered and the filtrate was left undisturbed to slowly evaporate. After 5 days, black crystals were obtained in ca. 10% yield (based on Mn). Elemental analysis (%) Calcd for [Mn<sup>III</sup><sub>4</sub>Mn<sup>II</sup><sub>2</sub>K<sub>2</sub>(L<sub>1</sub>)<sub>4</sub>(HL<sub>1</sub>)<sub>2</sub>(oxa)(H<sub>2</sub>O)<sub>4</sub>] (C<sub>110</sub>H<sub>80</sub>K<sub>2</sub>Mn<sub>6</sub>N<sub>6</sub>O<sub>26</sub>): C 57.15, H 3.46, N 3.64; found: C 58.01, H 3.66, N 3.42.

#### **Preparation of [Mn<sup>III</sup><sub>3</sub>(L<sub>1</sub>)<sub>2</sub>(HL<sub>1</sub>)(acac)]·(solvent)<sub>x</sub> (compound 2)**

Mn(acac)<sub>3</sub> (317mg, 0.9mmol), H<sub>3</sub>L<sub>1</sub> (176mg, 0.6mmol), and KHCO<sub>3</sub> (180mg, 1.8mmol) were solved in CH<sub>3</sub>OH (20mL) and stirred for 2 h under Ar protected. The resulting dark solution was then filtered and the filtrate was left undisturbed in glove box. After 3 days, black crystals were obtained in ca. 43% yield (based on Mn). Elemental analysis (%) Calcd for [Mn<sup>III</sup><sub>3</sub>(L<sub>1</sub>)<sub>2</sub>(HL<sub>1</sub>)(acac)] (C<sub>59</sub>H<sub>44</sub>Mn<sub>3</sub>N<sub>3</sub>O<sub>11</sub>): C 62.34, H 3.87, N 3.70. Found: C 60.59, H 4.36, N 3.34.

#### **Preparation of [Mn<sup>III</sup>Mn<sup>II</sup><sub>2</sub>(L<sub>2</sub>)<sub>2</sub>(acac)<sub>2</sub>(OAc)]·(solvent)<sub>x</sub> (compound 3)**

Mn(acac)<sub>3</sub> (317mg, 0.9mmol), H<sub>2</sub>L<sub>2</sub> (167mg, 0.6mmol), and KHCO<sub>3</sub> (180mg, 1.8mmol) were added into a solution of CH<sub>3</sub>CN (16mL) and DMF (4mL). After stirring for 2 h, the resulting dark solution was filtered and the filtrate was left undisturbed to slowly evaporate. After 3 days, black crystals were obtained in ca. 38% yield (based on Mn). Elemental analysis (%) Calcd for [Mn<sup>III</sup>Mn<sup>II</sup><sub>2</sub>(L<sub>2</sub>)<sub>2</sub>(acac)<sub>2</sub>(OAc)] (C<sub>46</sub>H<sub>41</sub>Mn<sub>3</sub>N<sub>4</sub>O<sub>10</sub>): C 56.64, H 4.21, N 5.75. Found: C 56.03, H 4.33, N 5.72.

#### **Derivatization experiment**

Derivatization experiment for carboxylic acid was operated according to the literature.<sup>6</sup> The solution of Mn(acac)<sub>3</sub> (317mg, 0.9mmol), ligand (176mg, 0.6mmol) and KHCO<sub>3</sub> (180mg, 1.8mmol) in 20mL CH<sub>3</sub>OH was removed the solvent at corresponding timeline. The residue was mixed with 3 mL 15% BF<sub>3</sub>/BuOH and 40 mL hexane in a 100mL round bottom flask and then was placed in a water bath at 70 °C for 1 h. After cooling, the reaction mixture was extracted with a mixture of 4 mL hexane, 12 mL water, and 1 mL acetonitrile. The extraction step was repeated twice and the resulting extracts were combined. The hexane layer was washed with four portions of 10 mL water and then dried with anhydrous Na<sub>2</sub>SO<sub>4</sub>. The filtrate was concentrated by rotary

evaporation to ~5mL, filtered through a PTFE syringe filter and then 3mg n-nonane was added as internal standard substance.

Formaldehyde (HCHO) is reacted with 2,4-dinitrophenylhydrazine (DNPH) to form a Schiff base (HCHO-DNPH derivatization product), which has an absorbing maximum ( $\lambda_{\max}$ ) at 360 nm.<sup>7</sup> To a 50mL flask, 20mg (DNPH) was solved in 10mL CH<sub>3</sub>OH, added with 1mL HCl (10N). Then 10mL mother liquid was added, reacted in 50°C water bath with stirring for 30min. UV-Vis was conducted after diluting.

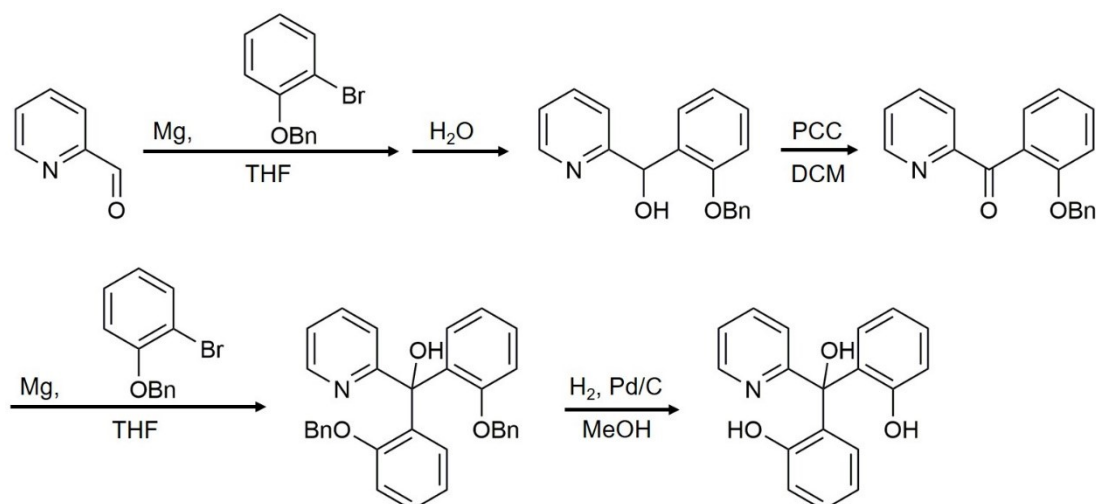
**Calculation:**

The yield of oxalate was calculated according to the equation:

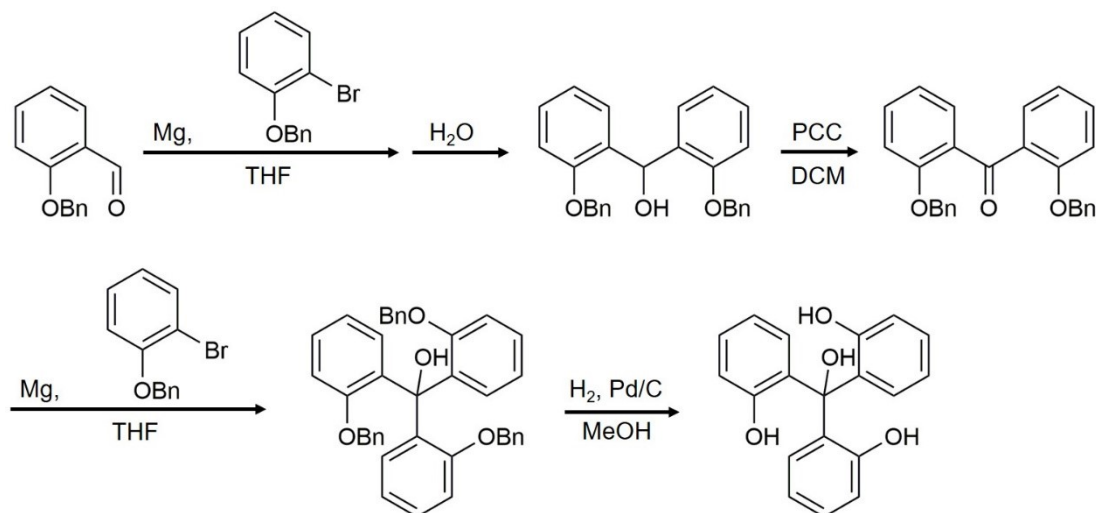
$$\eta = \frac{6n_{oxa}}{n_{ligand}} \times 100\%$$

( $n_{oxa}$ : molar amount of oxalate;  $n_{ligand}$ : molar amount of H<sub>3</sub>L<sub>1</sub>.)

**Scheme S1.** Synthesis route of H<sub>3</sub>L<sub>1</sub>.



**Scheme S2.** Synthesis route of H<sub>4</sub>L<sub>3</sub>.



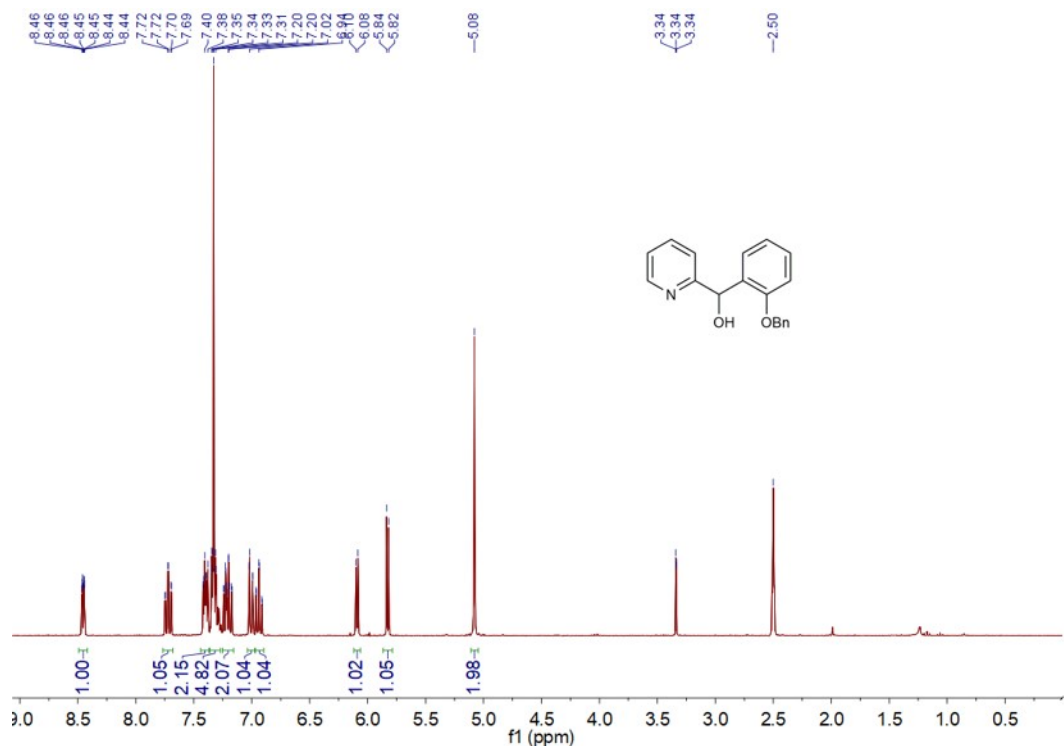


**Fig. S1** The  $^1\text{H}$  NMR (300 MHz,  $\text{DMSO-d}_6$ , 25  $^\circ\text{C}$ ) data of (2-(benzyloxy)phenyl)(pyridin-2-yl)methanol. The peaks of 3.33 and 2.5 correspond to H atoms of  $\text{H}_2\text{O}$  and DMSO respectively.

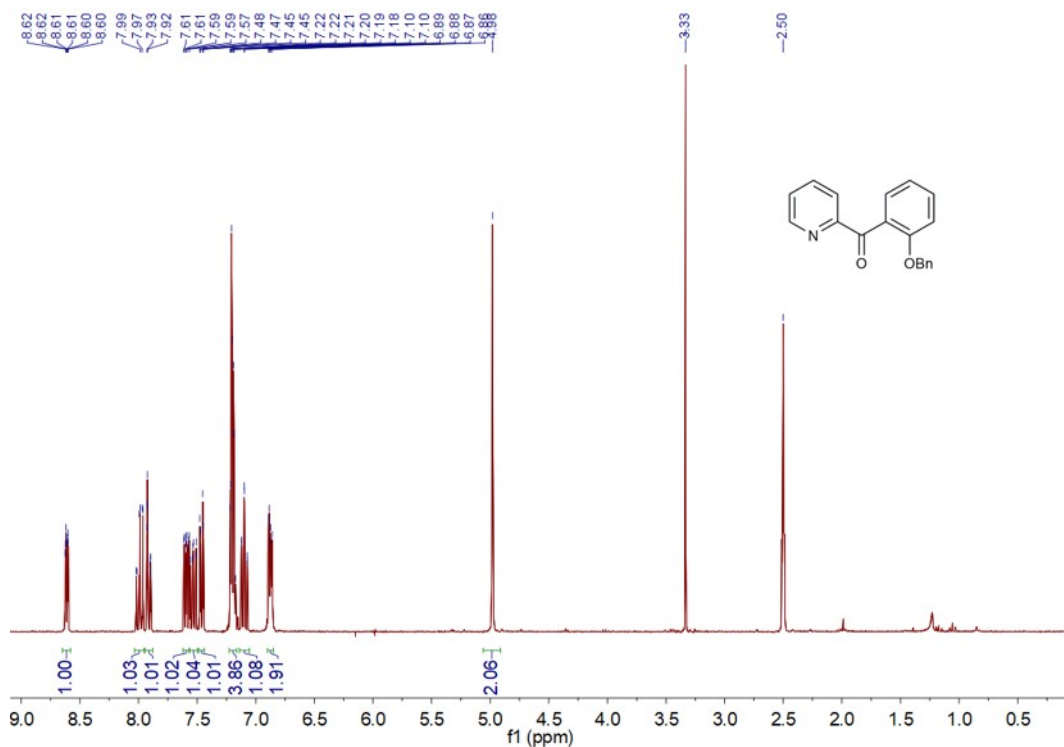


**Fig. S2** The  $^1\text{H}$  NMR (300 MHz,  $\text{DMSO-d}_6$ , 25  $^\circ\text{C}$ ) data of (2-(benzyloxy)phenyl)(pyridin-2-yl)methanone. The peaks of 3.33 and 2.5 correspond to H atoms of  $\text{H}_2\text{O}$  and DMSO respectively.

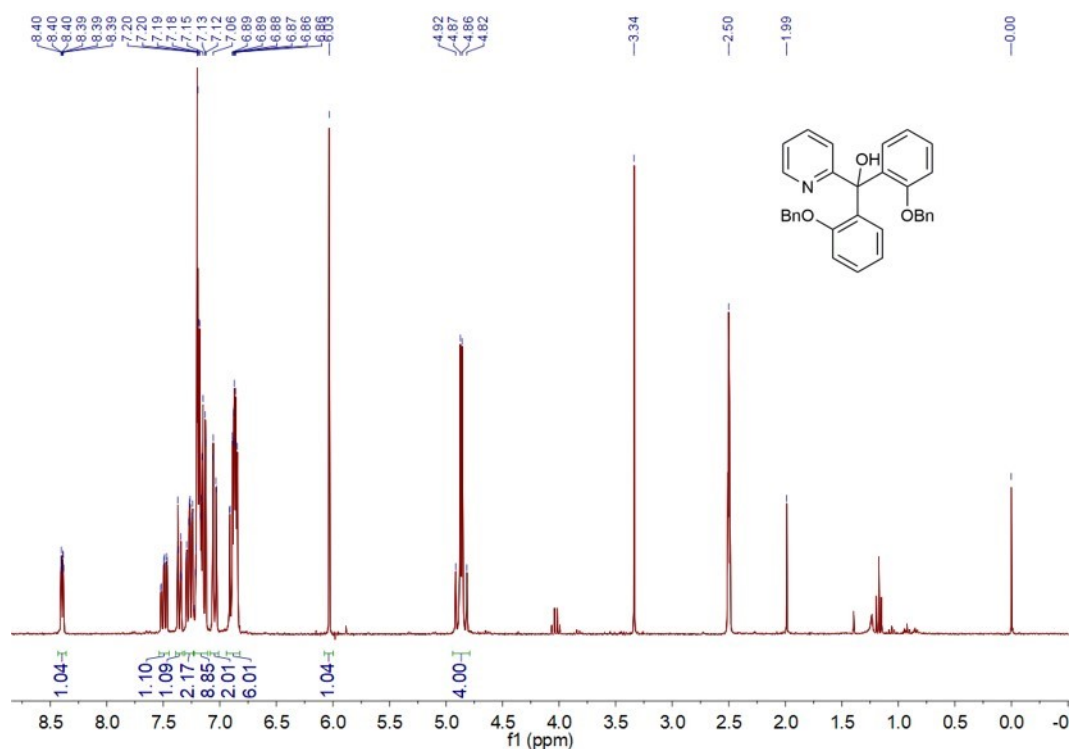


**Fig. S3** The  $^1\text{H}$  NMR (300 MHz,  $\text{DMSO-d}_6$ , 25  $^\circ\text{C}$ ) data of bis(2-(benzyloxy)phenyl)(pyridin-2-yl)methanol. The peaks of 3.33 and 2.5 correspond to H atoms of  $\text{H}_2\text{O}$  and DMSO respectively.

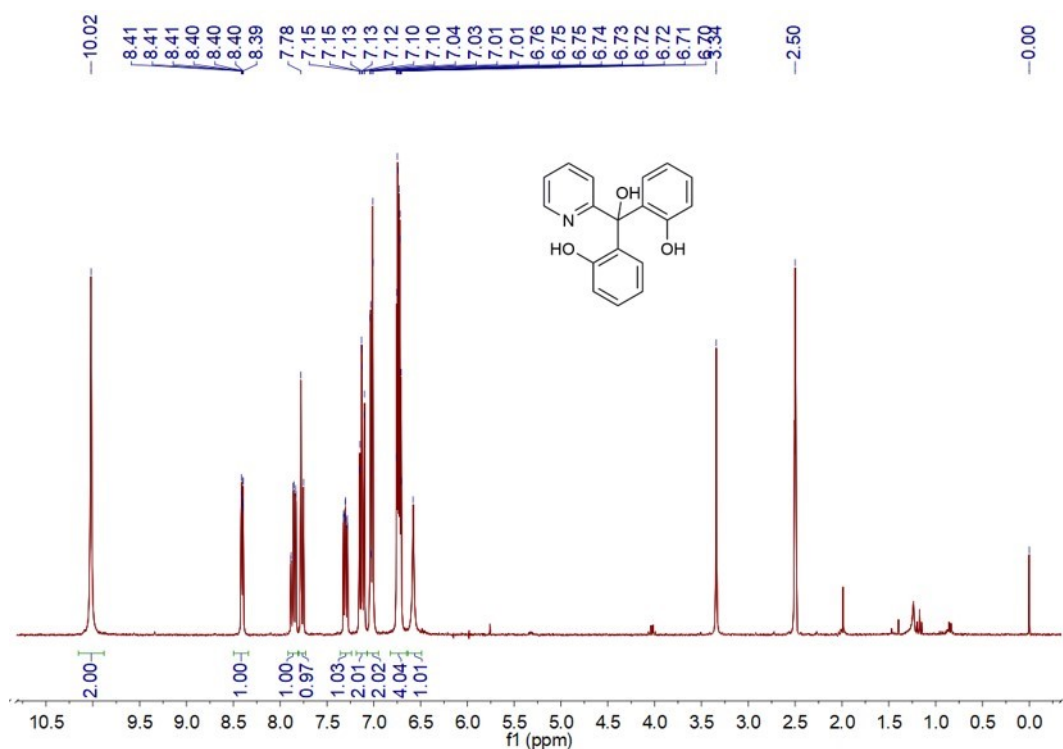


**Fig. S4** The  $^1\text{H}$  NMR (300 MHz,  $\text{DMSO-d}_6$ , 25  $^\circ\text{C}$ ) data of ligand  $\text{H}_3\text{L}_1$ . The peaks of 3.33 and 2.5 correspond to H atoms of  $\text{H}_2\text{O}$  and DMSO respectively.

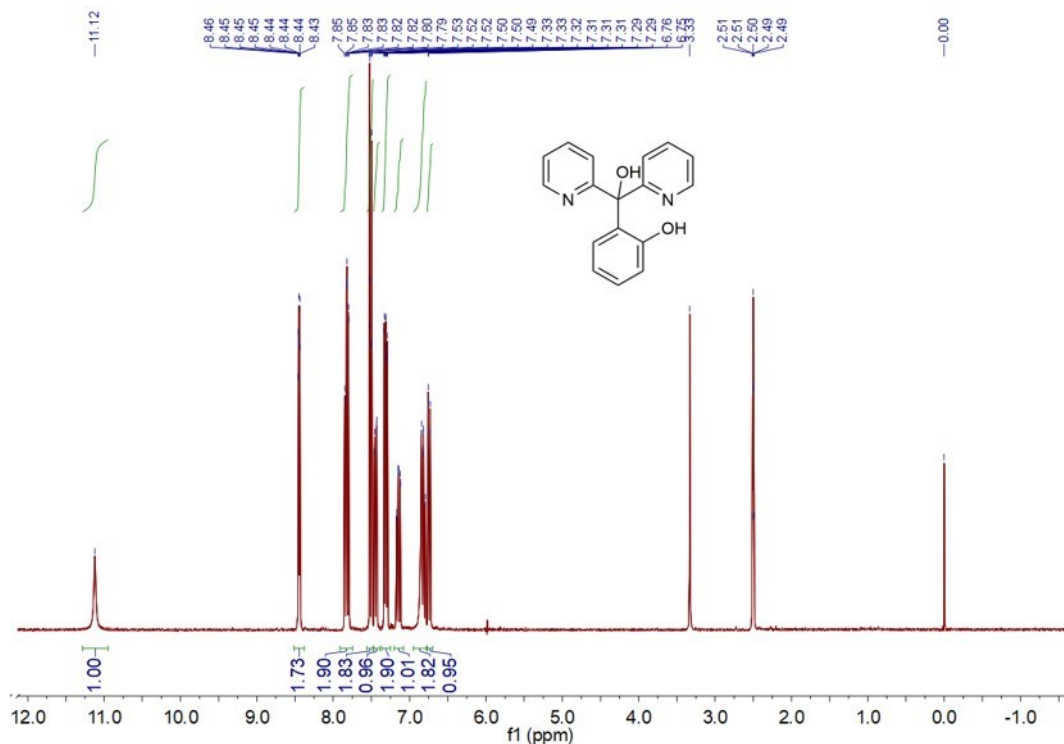


**Fig. S5** The  $^1H$  NMR (300 MHz, DMSO- $d_6$ , 25 °C) data of ligand  $H_2L_2$ . The peaks of 3.33 and 2.5 correspond to H atoms of  $H_2O$  and DMSO respectively.

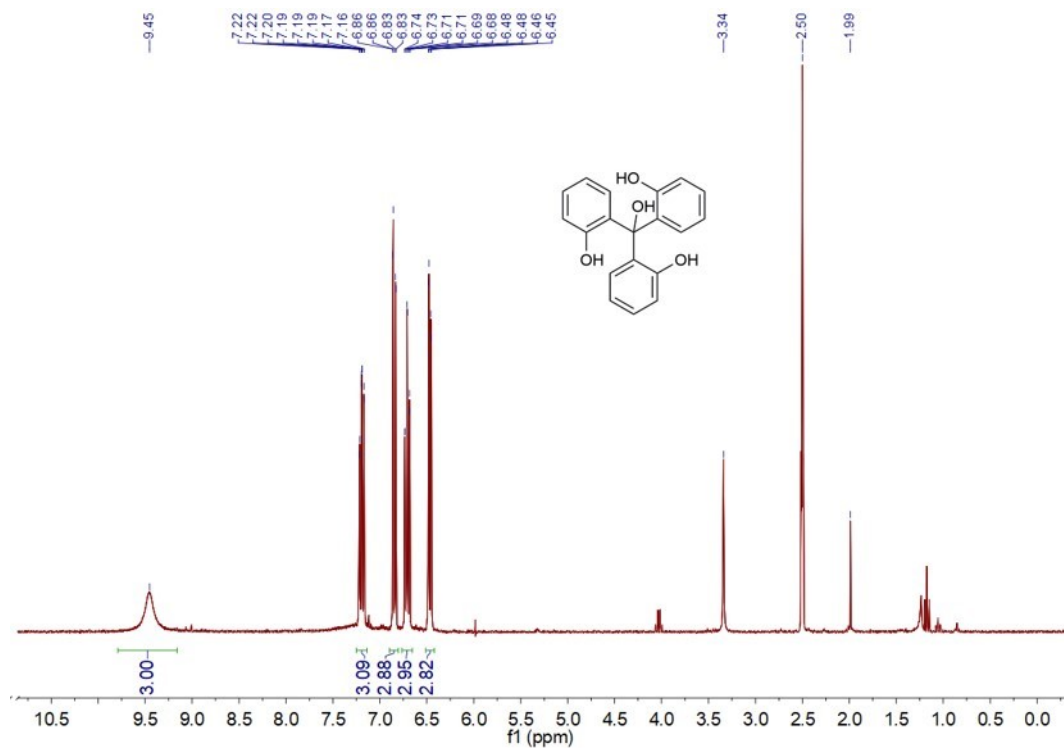


**Fig. S6** The  $^1H$  NMR (300 MHz, DMSO- $d_6$ , 25 °C) data of ligand  $H_4L_3$ . The peaks of 3.33 and 2.5 correspond to H atoms of  $H_2O$  and DMSO respectively.

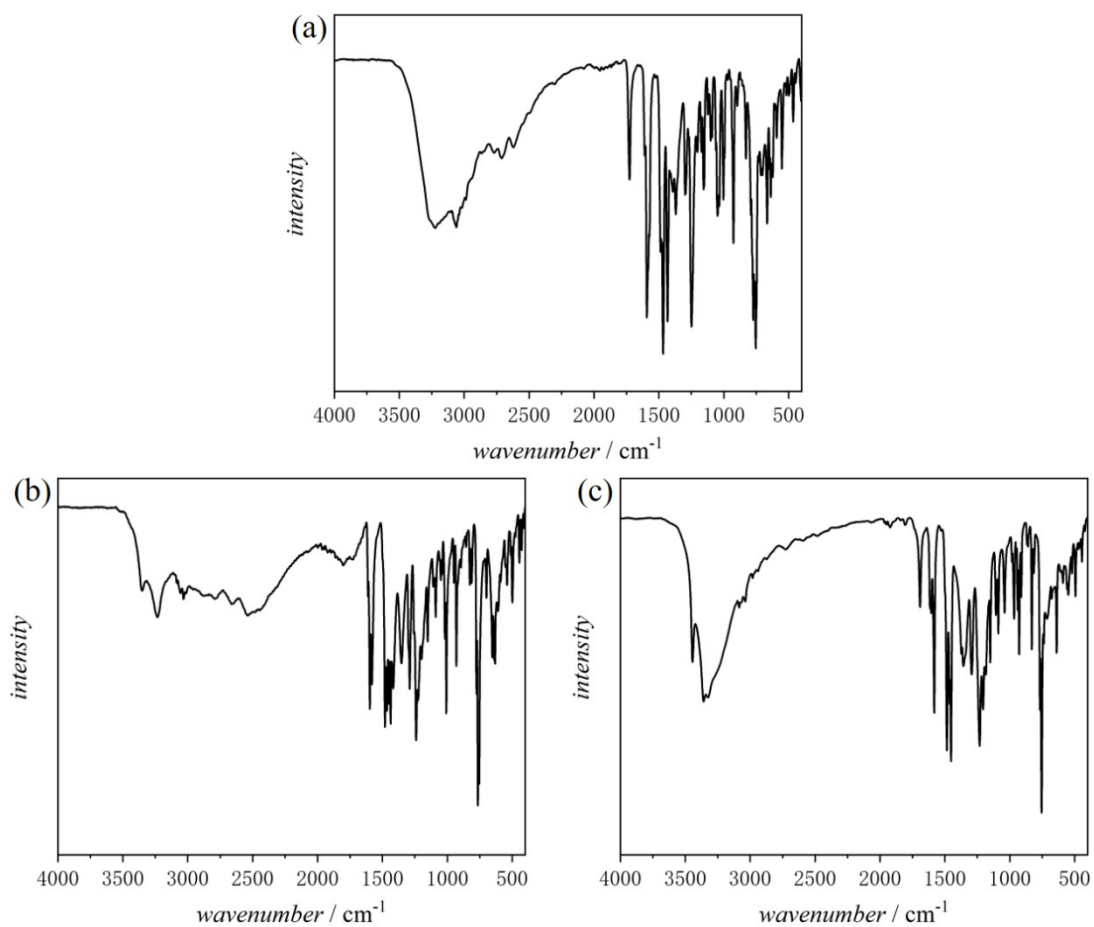


**Fig. S7** FT-IR spectra of H<sub>2</sub>L<sub>2</sub> (a), H<sub>3</sub>L<sub>1</sub> (b), and H<sub>4</sub>L<sub>3</sub> (c).

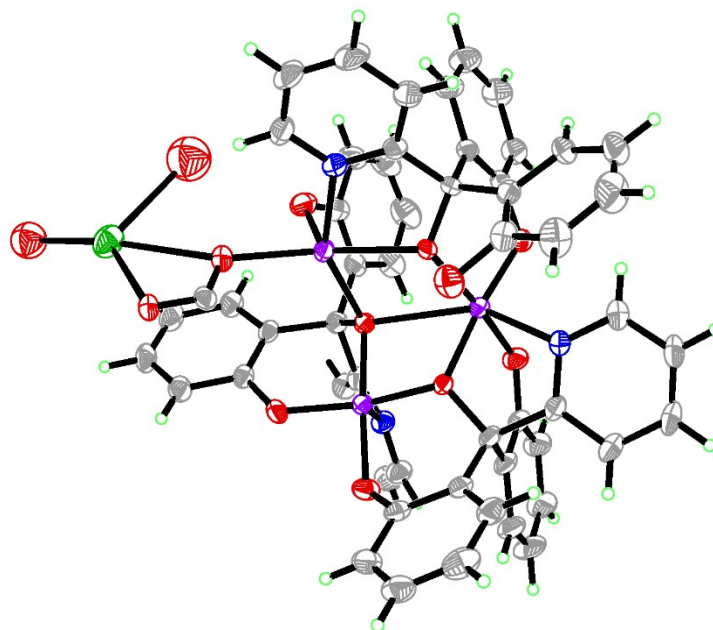


**Fig. S8** ORTEP plots of the asymmetric unit of compound **1**. Displacement ellipsoids are drawn at the 30% probability level. (Mn: purple; O: red; N: blue; C: grey; K: green)



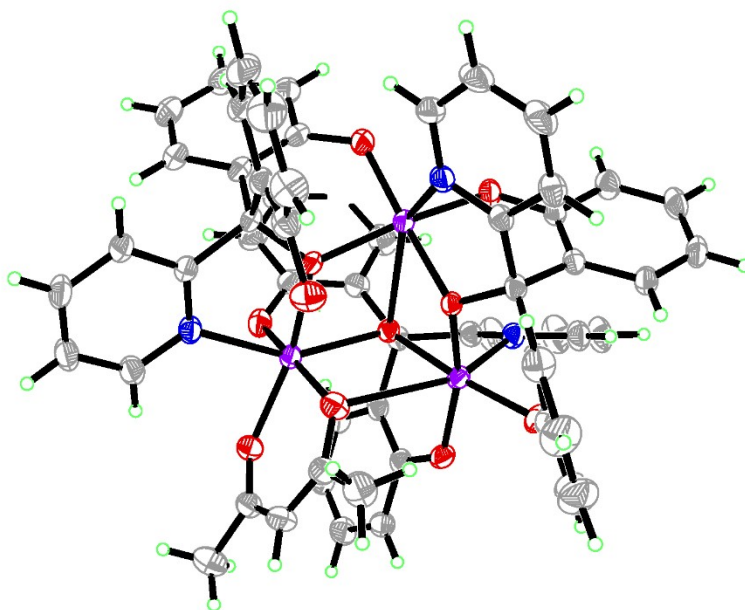


**Fig. S9** ORTEP plots of the asymmetric unit of compound **2**. Displacement ellipsoids are drawn at the 30% probability level. (Mn: purple; O: red; N: blue; C: grey)

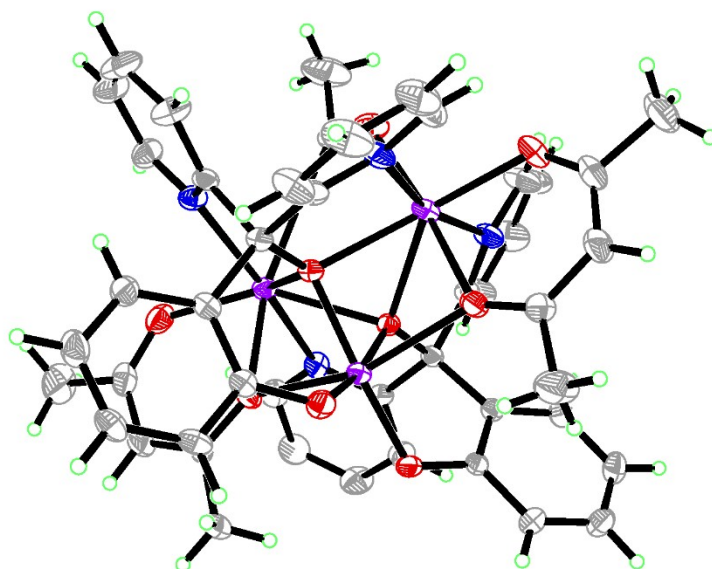


**Fig. S10** ORTEP plots of the asymmetric unit of compound **3**. Displacement ellipsoids are drawn at the 30% probability level. (Mn: purple; O: red; N: blue; C: grey)

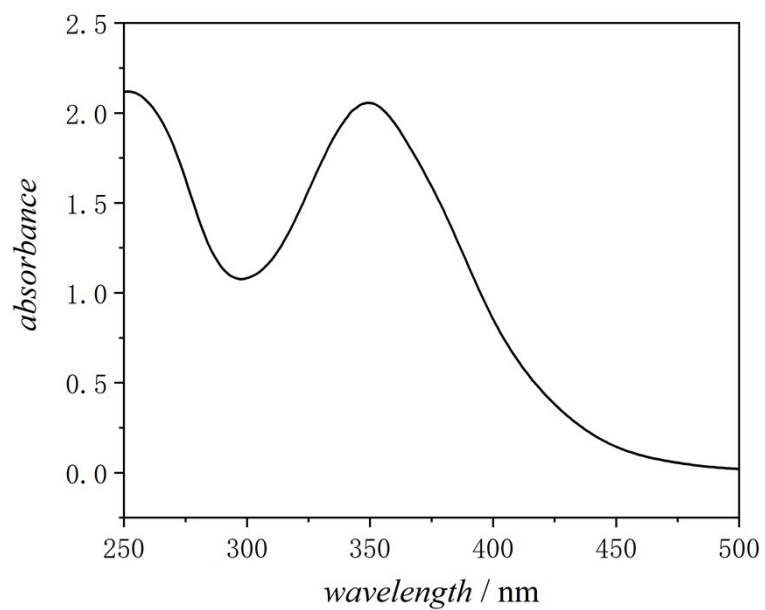


**Fig. S11** UV-vis spectra of derivatization product of formaldehyde.

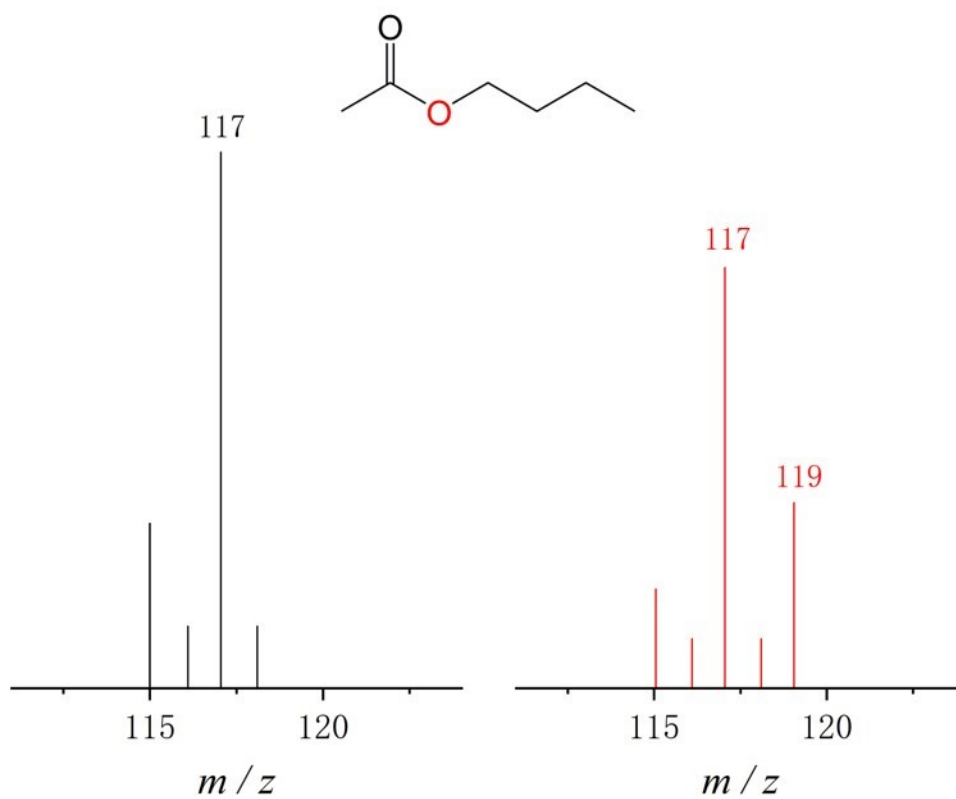


**Fig. S12** GC-MS spectra of butyl acetate with  $^{16}\text{O}$  (left) and  $^{18}\text{O}$  (right).

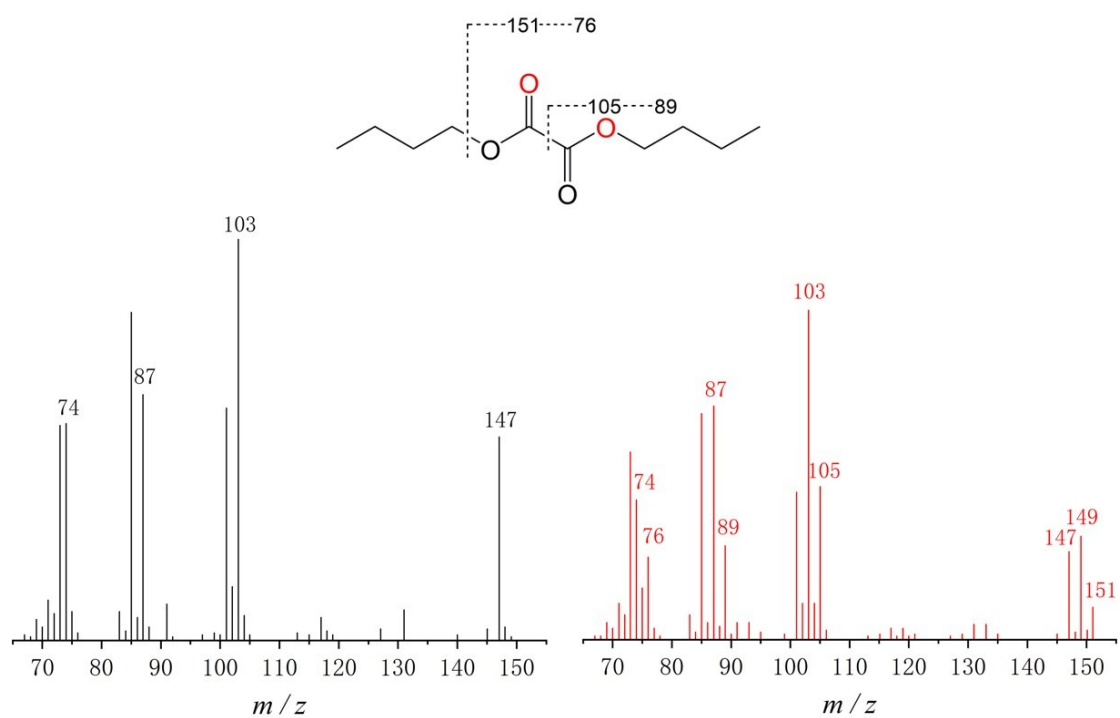


**Fig. S13** GC-MS spectra of dibutyl oxalate with  $^{16}\text{O}$  (left) and  $^{18}\text{O}$  (right).

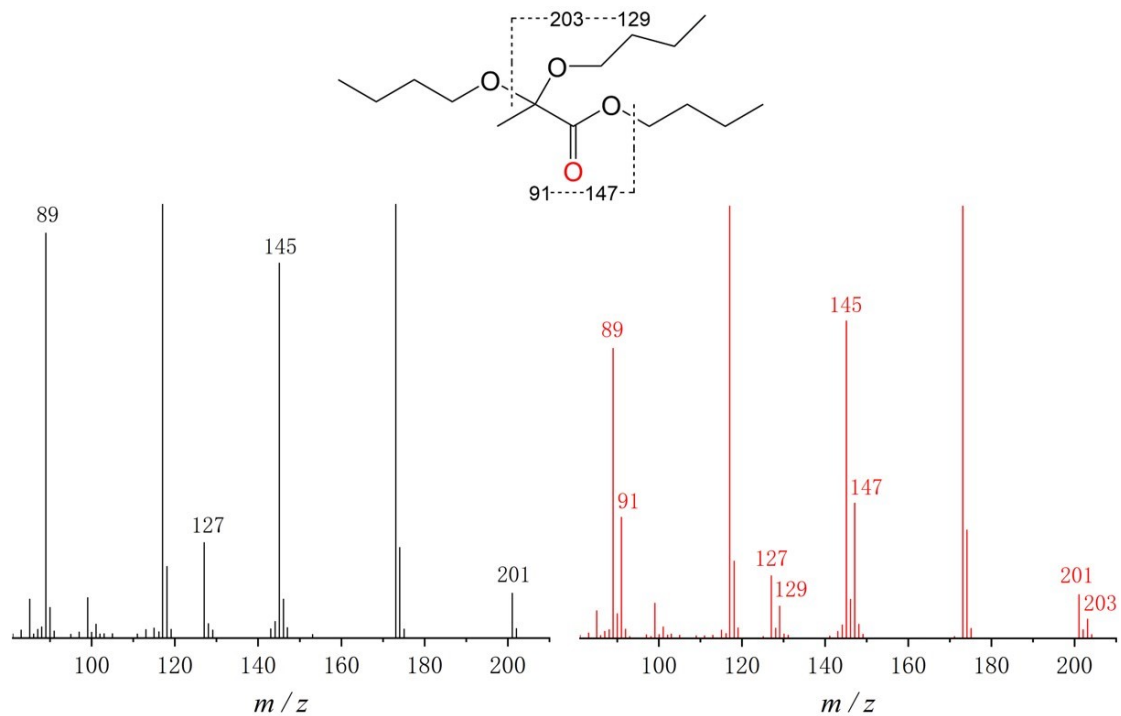


**Fig. S14** GC-MS spectra of butyl pyruvate with  $^{16}\text{O}$  (left) and  $^{18}\text{O}$  (right).

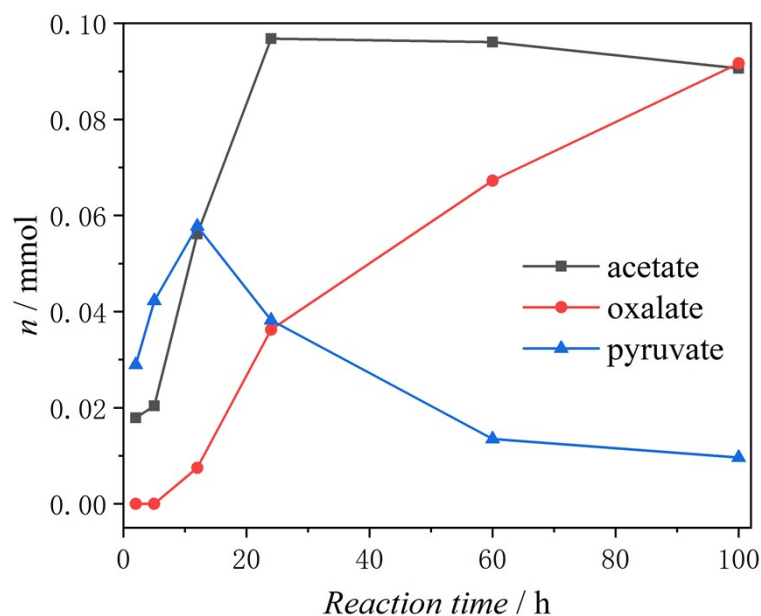


**Fig. S15** Time-dependent amount of the oxidative cleavage product.

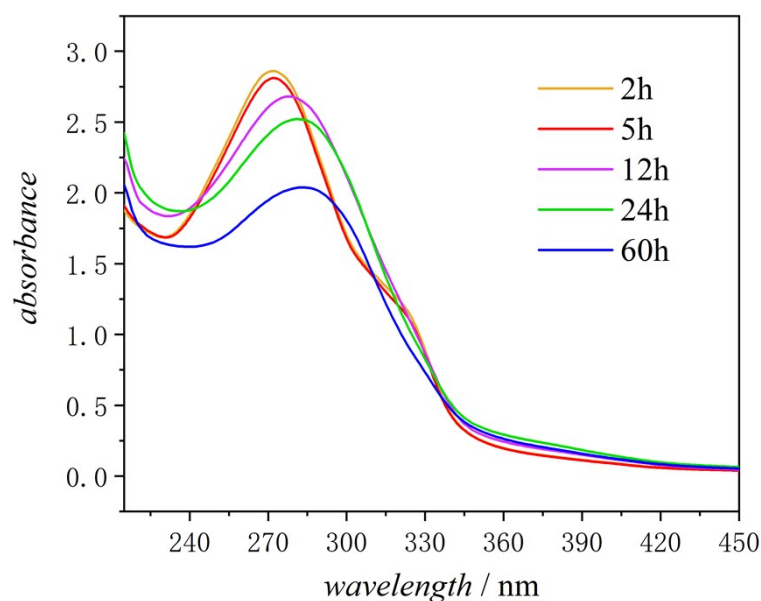


**Fig. S16** The time-dependent UV-vis spectra of the reaction mixture upon  $O_2$  exposure, showing a steady decrease in the absorption at around 280nm, which is ascribed to the LMCT of Mn(III) involving the phenolate ligands. This result indicated the spontaneous reduction of Mn(III) to Mn(II) over the oxalate complex in the oxidative cleavage pathway.

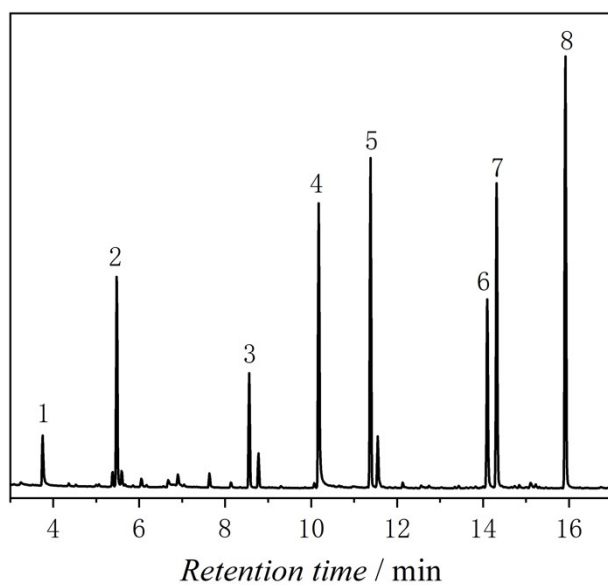


**Fig. S17** GC-MS spectra of the derivative sample of  $\text{Mn}(\text{acac})_3$ ,  $\text{H}_2\text{L}_2$ , and  $\text{KHCO}_3$  in  $\text{CH}_3\text{CN}$  exposed to  $\text{O}_2$  for 60h. (1: butyl acetate; 2: internal standard substance; 5: 1,1-dibutoxybutane, which may form from the reaction of butanol and  $\text{Mn}^{\text{III}}$ ; 8: butyl pyruvate; 3,4,6,7 are undefined substances; no dibutyl oxalate was detected.)

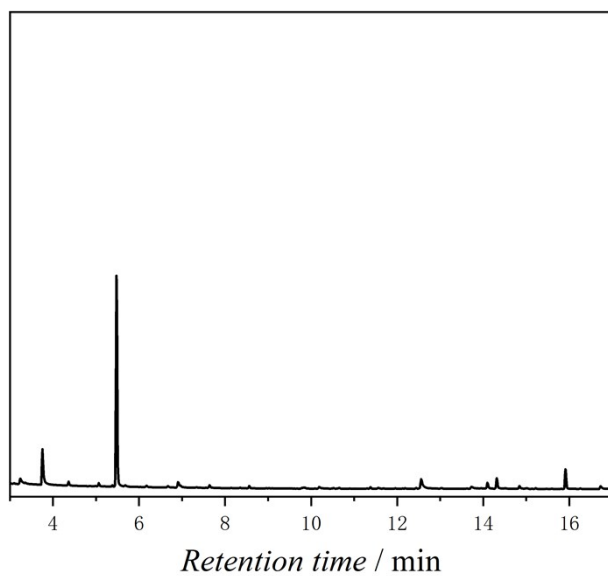


**Fig. S18** GC-MS spectra of the derivative sample of  $\text{Mn}(\text{acac})_3$ ,  $\text{H}_4\text{L}_3$ , and  $\text{KHCO}_3$  in  $\text{CH}_3\text{CN}$  exposed to  $\text{O}_2$  for 60h.

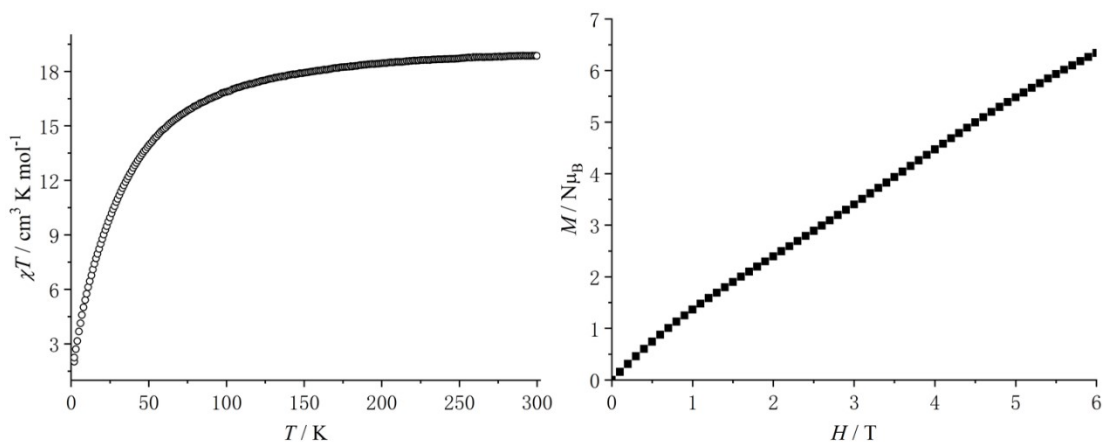


**Fig. 19**  $\chi T$  vs.  $T$  plot under 1000 Oe dc field (left) and isothermal magnetization curve at 2 K (right) for compound **1**.

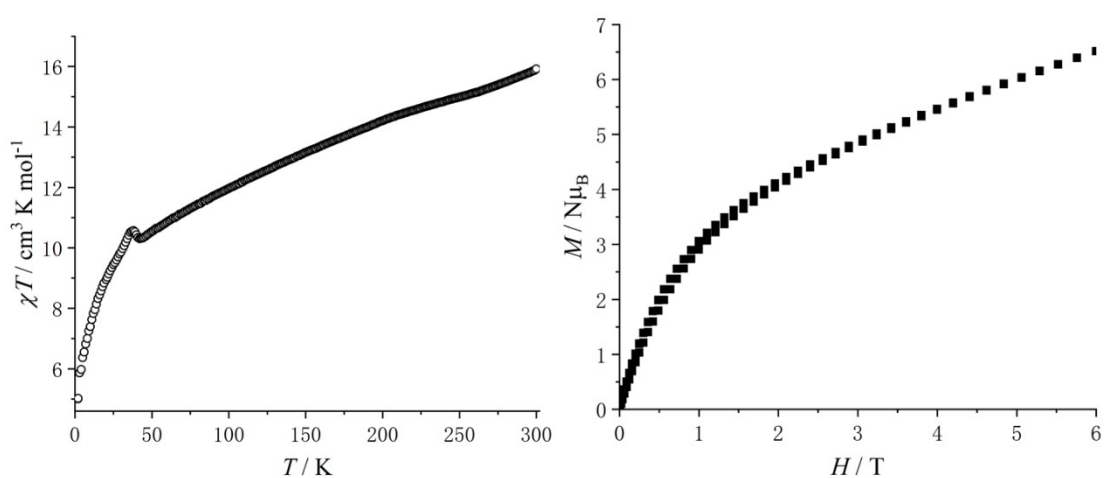


**Fig. 20**  $\chi T$  vs.  $T$  plot under 1000 Oe dc field (left) and isothermal magnetization curve at 2 K (right) for compound **2**.

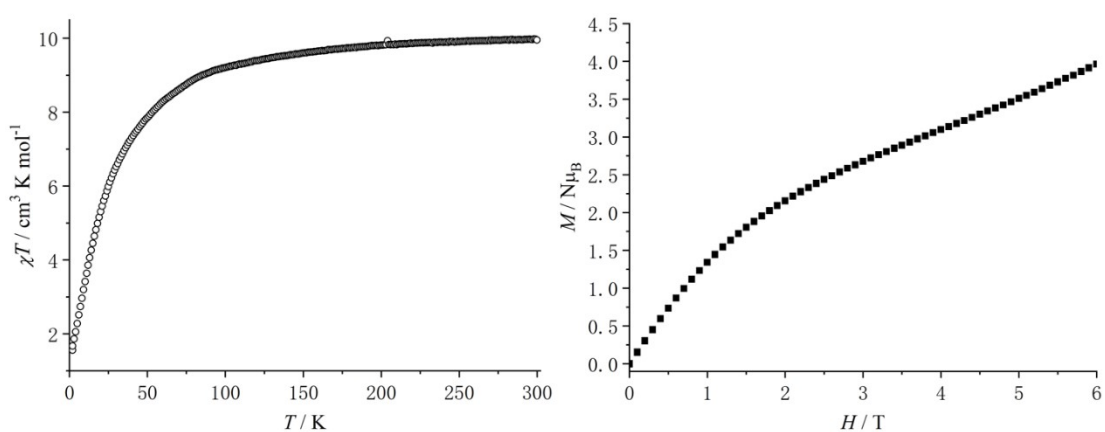


**Fig. 21**  $\chi T$  vs.  $T$  plot under 1000 Oe dc field (left) and isothermal magnetization curve at 2 K (right) for compound **3**.

**Table S1** Crystallographic data for **1**, **2** and **3**

compound	1	2	3
Empirical formula	C <sub>110</sub> H <sub>80</sub> K <sub>2</sub> Mn <sub>6</sub> N <sub>6</sub> O <sub>26</sub>	C <sub>59</sub> H <sub>44</sub> Mn <sub>3</sub> N <sub>3</sub> O <sub>11</sub>	C <sub>46</sub> H <sub>41</sub> Mn <sub>3</sub> N <sub>4</sub> O <sub>10</sub>
Formula weight	2309.64	1135.79	974.65
Temperature / K	273.15	299.62	273.15
Crystal system	monoclinic	monoclinic	monoclinic
Space group	<i>P</i> 2 <sub>1</sub> / <i>n</i>	<i>P</i> 2 <sub>1</sub> / <i>c</i>	<i>P</i> 2 <sub>1</sub> / <i>n</i>
<i>a</i> / Å	14.139(3)	16.3760(7)	10.833(2)
<i>b</i> / Å	22.693(5)	14.9059(7)	37.692(8)
<i>c</i> / Å	16.025(3)	25.2682(10)	11.684(3)
$\alpha$ / °	90	90	90
$\beta$ / °	95.846(7)	107.6090(10)	91.393(7)
$\gamma$ / °	90	90	90
Volume / Å <sup>3</sup>	5115.1(19)	5878.9(4)	4769.1(17)
<i>Z</i>	2	4	4
$\rho_{\text{calc}}$ / g / cm <sup>3</sup>	1.500	1.283	1.357
$\mu$ / mm <sup>-1</sup>	0.880	0.693	0.840
<i>F</i> (000)	2356.0	2328.0	2000.0
Crystal size / mm <sup>3</sup>	0.150 × 0.120 × 0.110	0.140 × 0.130 × 0.110	0.140 × 0.130 × 0.110
Radiation	MoK $\alpha$ ( $\lambda$ = 0.71073)	MoK $\alpha$ ( $\lambda$ = 0.71073)	MoK $\alpha$ ( $\lambda$ = 0.71073)
2 $\theta$ range for data collection / °	3.122 to 51.506	4.858 to 49.512	4.762 to 50.238
Index ranges	-16 ≤ <i>h</i> ≤ 16, -27 ≤ <i>k</i> ≤ 27, -19 ≤ <i>l</i> ≤ 19	-19 ≤ <i>h</i> ≤ 18, -17 ≤ <i>k</i> ≤ 15, -29 ≤ <i>l</i> ≤ 29	-12 ≤ <i>h</i> ≤ 12, -43 ≤ <i>k</i> ≤ 45, -13 ≤ <i>l</i> ≤ 13
Reflections collected	42300	34537	53128
Independent reflections	9237 [R <sub>int</sub> = 0.0882, R <sub>sigma</sub> = 0.0774]	10005 [R <sub>int</sub> = 0.0297, R <sub>sigma</sub> = 0.0300]	8461 [R <sub>int</sub> = 0.1166, R <sub>sigma</sub> = 0.0713]
Data / restraints / parameters	9237/0/678	10005/0/688	8461/0/573
Goodness-of-fit on <i>F</i> <sup>2</sup>	1.056	1.029	1.050
Final <i>R</i> indexes [ <i>I</i> ≥ 2 $\sigma$ ( <i>I</i> )]	<i>R</i> <sub>1</sub> = 0.0765, w <i>R</i> <sub>2</sub> = 0.2356	<i>R</i> <sub>1</sub> = 0.0332, w <i>R</i> <sub>2</sub> = 0.0829	<i>R</i> <sub>1</sub> = 0.0607, w <i>R</i> <sub>2</sub> = 0.1556
Final <i>R</i> indexes [all data]	<i>R</i> <sub>1</sub> = 0.1079, w <i>R</i> <sub>2</sub> = 0.2589	<i>R</i> <sub>1</sub> = 0.0433, w <i>R</i> <sub>2</sub> = 0.0886	<i>R</i> <sub>1</sub> = 0.0980, w <i>R</i> <sub>2</sub> = 0.1717
Largest diff. peak / hole / e Å <sup>-3</sup>	1.37/-0.91	0.22/-0.28	0.40/-0.44

## References

- [1] G. M. Sheldrick, *Acta Crystallogr., Sect. A: Found. Adv.* 2015, **71**, 3-8.
- [2] G. M. Sheldrick, SHELXL-97: Program for x-ray crystal structure refinement; University of Gottingen: Gottingen, Germany, 1997.
- [3] Dolomanov, O. V.; Bourhis, L. J.; Gildea, R. J.; Howard, J. A. K.; Puschmann, H., *J. Appl. Crystallogr.*, 2009, **42**, 339-341.
- [4] Y. Zhang, C. Yang, F. Sun, G. Wu and S. Qiu, *Inorg. Chem. Commun.*, 2019, **106**, 6-10.
- [5] T. Saha, M. S. L. Kumar, S. Bera, B. B. Karkara, G. Panda, *RSC. Adv.*, 2017, **7**, 6966-6971.
- [6] Y. Li and J. Yu, *Environ. Sci. Technol.*, 2005, **39**, 7616-7624.
- [7] A. Soman<sup>1</sup>, Y. Qiu, and Q. Chan Li, *J. Chromatogr. Sci.*, 2008, **46**, 461-465.